ORIGINAL PAPER

Codeposition of copper and tin from acidic sulfate solutions containing polyethylene glycols. Effect of length of the hydrocarbon chain

Arvydas Survila · Dalia Bražinskienė · Stasė Kanapeckaitė · Zenius Mockus · Vitalija Jasulaitienė

Abstract Voltammetry and electrochemical impedance spectroscopy technique were applied to study the effect of polyethylene glycols (PEG) with different molecular mass on Cu(II) and Sn(II) reduction kinetics in acidic sulfate solutions. Tetraethylene glycol was found to be the surface-active oligomer on both Cu and Sn substrates that holds the shortest $(-CH_2-CH_2-O-)_m$ chain. The exchange current density of the rate-limiting step $Cu^{2+} + e \rightarrow Cu^+$ falls drastically with an increase in the molecular mass of PEG. An addition of PEG into halide-free Sn(II) solutions results in the significant inhibition of Sn(II) reduction in the entire range of cathodic polarizations including the region of limiting current. Inhibition degree also increases with PEG molecular mass. In contrast with Cu|Cu(II) system, formation of adsorption layers on Sn electrodes proceeds significantly slower. Underpotential deposition of Sn(II) is observed in the region of Cu(II)-limiting current. The characteristic current minimum arises in the region where free Sn phase is thermodynamically stable. It deepens with the length of the hydrocarbon chain of PEG. The fall of current density seems to arise from the inhibitive PEG adsorption on tin atoms that are still not incorporated into general Cu–Sn lattice.

Keywords Copper · Tin · Codeposition · Polyethylene glycol · Adsorption · Impedance

A. Survila (✉) · D. Bražinskienė · S. Kanapeckaitė · Z. Mockus · V. Jasulaitienė
Institute of Chemistry,
A. Goštauto 9,
01108 Vilnius, Lithuania
e-mail: arvydass@ktl.mii.lt

Introduction

Copper–tin alloys are among the most beneficial coatings that are used for various purposes. They show good solderability, malleability, and ductility and have good corrosion resistance. Besides, the coatings known as yellow bronze (containing 10–20 mass percent of tin) confer excellent decorative properties to the substrate. To obtain the desired characteristics of bronze coatings, the control of Cu and Sn codeposition is of fundamental importance. For this purpose, different polyethers, including polyethylene glycols (PEG), that operate in combination with some other organic compounds (brighteners, stabilizators, etc) are widely employed in modern plating industry.

Most researches have shown that polyethers reduce the rate of copper deposition. Several mechanisms of PEG action have been proposed [1–8] including the role of chlorides that assist in the suppression of Cu(II) reduction. More exhaustive investigations in this field have shown [9–11] that halides enhance the inhibition activity of halides in the series: $Cl^- < Br^- < I^-$. In contrast, polyethers exhibit strong inhibitive adsorption on tin substrate and the effect of halides is quite opposite: they suppress the action of polyethers according to the above sequence [10–12].

Investigations involving PEG of different molecular masses have shown that the halide-enhanced inhibitive adsorption on copper depends not only on PEG concentration [4] but also on the length of hydrocarbon chain [13]. According to Hebert et al. [8], suppression of copper electrodeposition requires a polymer molar mass of at least ~1,000 g/mol and the presence of Cl^- ions at a concentration of the order of 1 mM. Pearson and Dennis [14] investigated some copolymers of ethene and propene oxides with molecular masses equal to 18,000, 50,000,

and 92,000. They found that the second surface-active substance (SAS) suppresses Cu(II) reduction to the most extent. A somewhat similar conclusion has been made by Dow et al. [15] who investigated the influence of PEG on the microvia filling by copper electroplating. They found that the best performance of plating formula was obtained when molecular mass was not too high and ranged from 6,000 to 8,000.

Recently, we have found that too short PEG molecules cannot be classified as SAS overall [16–18]. For instance, no perceptible inhibition has been observed in Cu(II) solutions involving monoethylene (EG), diethylene, or triethylene glycols even in the presence of halides [16, 17]. Only tetraethylene glycol (TEG) HO–$(CH_2$–CH_2–O$)_4$–H or other PEGs with higher molecular mass can give rise for inhibition of Cu(II) reduction.

Undoubtedly, the length of hydrocarbon chain is one of the factors that play an important role in the electrode processes. However, the literature data concerning this area are few in number yet. We undertake the present investigation in order to establish the most general regularities regarding the influence of ethylene glycol and its polymeric derivatives HO–$(CH_2$–CH_2–O$)_m$–H on the kinetics of Cu(II) and/or Sn(II) reduction. An attempt is made to involve a sufficiently wide range of molecular mass, beginning with EG ($m=1$) and ending with PEG-40000 ($m\approx900$). Experimental data obtained by voltammetry and electrochemical impedance spectroscopy are presented and discussed in this article.

Experimental

Solutions were prepared using thrice-distilled water, $CuSO_4\cdot5H_2O$ (Mallinckrodt, USA, chlorides less than 0.005%), $SnSO_4$ (Fluka or Aldrich, chlorides less than 0.01%), H_2SO_4, and potassium halides (high purity, Reakhim Russia). Besides, different polyethers HO(CH_2–CH_2–O$)_m$–H were added into the 0.01 M Cu(II) or/and Sn (II) solutions. EG oligomers with $m\leq4$ were pure substances; other SAS were fractionated PEG mixtures with ~5–10% deviations from average molecular mass. Pure argon stream was passed through solutions for 0.5 h before measurements. Argon atmosphere was also kept under solutions throughout the experiments.

To prepare the working electrodes, platinum or gold substrates were coated with Cu or Sn in the solutions containing (g dm^{-3}): (a) $CuSO_4\cdot5$ H_2O 250, H_2SO_4 50; (b) $SnSO_4$ 60, H_2SO_4 160, laprol 1. Thickness of smooth coatings was 5–7 μm. The electrodes were rinsed with water, immediately immersed into solution under investigation, and kept in it for a controlled time τ. Besides, conventional three-electrode cells contained copper, tin, or bronze anode and Ag|AgCl|KCl(sat) reference electrode.

Electrode potentials E were converted to the standard hydrogen scale. All experiments were performed at 20 °C.

Rotating disc electrode (RDE) was used in voltammetric measurements that were performed at potential sweep rate, equal to 5 mV s^{-1}, using a potentiostat PI-50-1 (Russia). Fused glass holder Pt disk (1-cm^2 surface area) served as a substrate for the preparation of working electrodes.

Coated copper or tin Pt wire with a surface area of 0.36 cm^2 was used in electrochemical impedance spectroscopy (EIS). Impedance measurements were carried out under potentiostatic conditions at the open-circuit potentials within the frequency (f) range from 0.1 to 5×10^4 Hz using a Zahner Elektrik (Germany) IM6 Impedance Spectrum Analyzer. Each record took about 5 min and was repeated three to four times. Computer programs elaborated by Boukamp [19] were used for analyzing impedance spectra.

X-ray photoelectron spectroscopy was carried out using a Model ESCALAB-MKII spectrometer (for details, see [20]). Cu–Sn samples were prepared by electrolysis of the solutions at constant potential. The thickness of an analyzed layer was 1–2 nm. In some experiments, approximately 90-nm-thick surface layer was removed using the beam of Ar$^+$ ions.

Results and discussion

Electroreduction of Cu(II)

Voltammograms of Cu(II) reduction contain well-defined plateau of limiting current (i_d) that is of diffusive nature and obeys Nernst equation with $D=5.7\times10^{-6}$ cm^2 s^{-1}. Addition of various PEG into sulfate solutions exhibits rather weak influence on Cu(II) reduction kinetics. This may be seen from the example presented in Fig. 1. The results obtained are typical of most polyethers. Thus, to enhance the activity of these substances on copper substrate, a proper amount of halides should be introduced into solutions. By keeping this in mind, voltammetric investigations of copper electrodes were carried out with solutions containing chlorides or bromides. Unfortunately, procedures that are described bellow were not acceptable for iodide-containing solutions due to the emergence of current irregularities in the region of limiting current plateau.

Initial data regarding the effect of short PEG molecules have been reported in our previous paper [16]. It was established that EG oligomers containing less than three ethereal bonds show no surface activity even in the presence of halides. Thus, namely tetraethylene glycol is the surface-active oligomer in halide-containing solutions that holds the shortest hydrocarbon chain.

The main effect of TEG and other PEG with higher molecular mass consists in the certain increase in the cathodic polarization, but the limiting current remains on
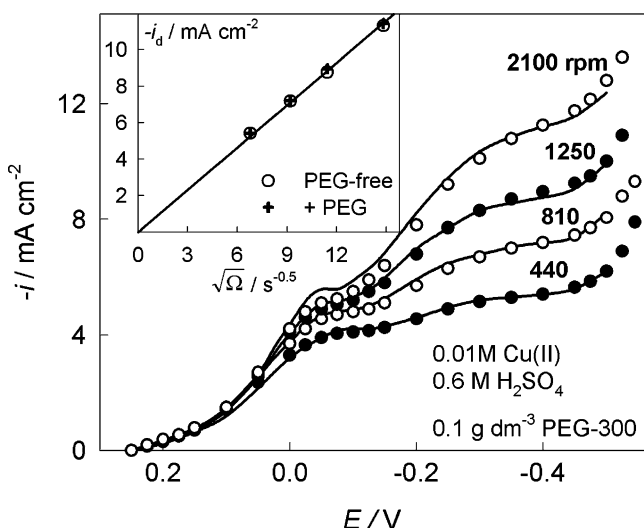
Fig. 1 Voltammograms of RDE obtained at indicated rotating velocities (revolutions per minute) for 0.01 M Cu(II) solutions without PEG (*lines*) and with PEG-300 (*symbols*). Limiting current densities taken at $E=-0.4$ V obey Levich equation with $D=5.7\times10^{-6}$ cm^2 s^{-1} (data in the *inset*). Ω is angular rotation velocity

the same level. In this case, the following analysis of voltammetric data is possible.

Considering that the reduction of Cu^{2+} ions proceeds by two one-electron transfers

$$Cu^{2+} + e \rightarrow Cu^{+}, \tag{1}$$

$$Cu^{+} + e \rightarrow Cu \tag{2}$$

and the net process is controlled by step (1) ($i_{01} << i_{02}$), the kinetic equation takes the form:

$$i = 2i_{01}\left\{\exp\left(\frac{(2-\alpha_{c1})F}{RT}\eta\right) - \frac{[Cu^{2+}]_s}{[Cu^{2+}]_b}\exp\left(-\frac{\alpha_{c1}F}{RT}\eta\right)\right\}. \tag{3}$$

were subscripts s and b denote the surface and bulk concentrations of Cu^{2+} ions. The former concentration is

dependent on the current density i according to the equation:

$$\frac{[Cu^{2+}]_s}{[Cu^{2+}]_b} = 1 - \frac{i}{i_d} \tag{4}$$

The linear relationship

$$\log\frac{-i}{1 - i/i_d} = \log 2i_{01} - \frac{\alpha_{c1}F}{2,303\,RT}\eta \tag{5}$$

following from Eqs. 3 and 4 at sufficiently high cathodic overvoltages, η, is specified further as normalized Tafel plot (NTP). Kinetic parameters of the process (1), viz. exchange current density i_{01} and cathodic charge transfer coefficient α_{c1}, were easily obtained from voltammetric data transformed according to the Eq. 5.

According to Bražinskienė and Survila [16, 17], addition of TEG results in the shift of NTP to lower values in a certain region of cathodic polarizations. However, when the certain potential is achieved, the destruction of adsorption layer is observed. This potential depends on the nature of halide and is equal to −0.02 and −0.1 V in the presence of Cl$^-$ and Br$^-$, respectively. Somewhat similar effects are also observed in the case of longer PEG molecules (Fig. 2), but the desorption of PEG was not observed in bromide-containing solutions up to −0.4 V.

Exchange current densities of Cu(II) stepwise reduction were also determined from impedance data using the equivalent circuit substantiated in [21]. It contains two parallel Faradaic subcircuits each of which involves charge transfer resistance R and Warburg impedance W in series. This set of elements is shunted with double-layer impedance, presented by the constant phase element Q_{dl}, and then the ohmic resistance of the solution Ω is added in series.

Fig. 2 Normalized Tafel plots obtained for Cu(II) and PEG-3000 solutions containing chlorides (*left part*) and bromides (*right part*)
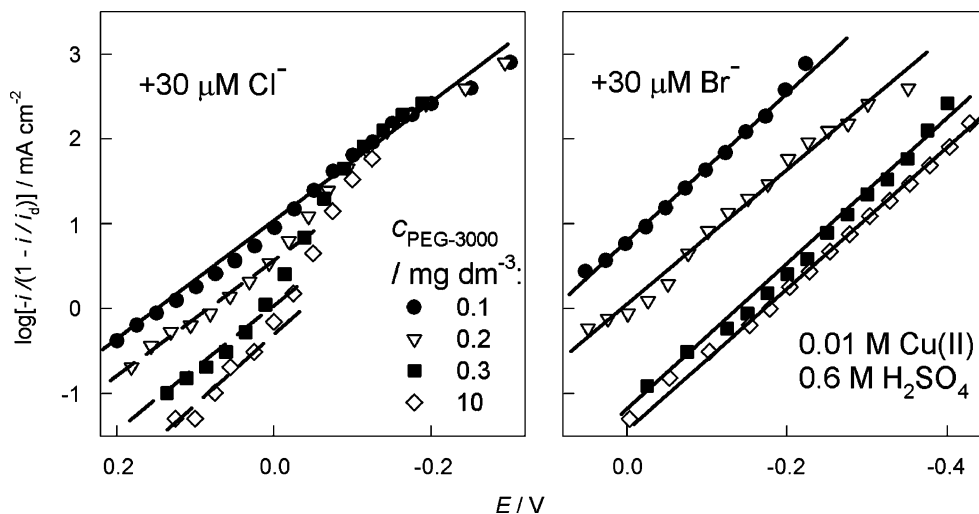
The following equations are valid for equilibrium conditions [21]:

$$i_{01} + i_{02} = \frac{RT}{F}\left(\frac{1}{R_1} + \frac{1}{R_2}\right), \qquad (6)$$

$$\frac{1}{i_{01}} + \frac{1}{i_{02}} = \frac{R_1 + R_2}{\sigma_1 + \sigma_2}\frac{1}{F\sqrt{D}}\left(\frac{1}{[Cu^{2+}]} + \frac{4}{[Cu^+]}\right), \qquad (7)$$

where σ_1 and σ_2 are coefficients of Warburg impedance (Z_W):

$$Z_W = \sigma(1-j)\big/\sqrt{\omega}, \qquad (8)$$

$j = \sqrt{-1}$, $\omega = 2\pi f$ and f is the frequency of alternating current.

Results presented in Fig. 3 show, firstly, that $i_{01} \ll i_{02}$; thus, the above conclusion regarding the nature of the rate-limiting step is confirmed. Secondly, i_{01} clearly depends on TEG concentration whereas i_{02} remains on the same level. Ultimately, it is evident that the inhibition of Cu(II) reduction is more pronounced in the bromide-containing solutions. It should be also noted that the open-circuit impedance of bromide-containing solutions steadies within 5–10 min whereas this duration takes at least 20 min in the presence of chlorides. Hence, the formation of adsorption layer occurs slower in the presence of chlorides.

A number of kinetic parameters obtained via NTP analysis of bromide-containing solutions are summarized in Table 1. It is clearly evident that the inhibition degree of Cu(II) reduction increases with PEG molecular mass. The exchange current density i_{01} falls drastically when the hydrocarbon chain lengthens, but the charge transfer coefficient α_{c1} remains within the limits from 0.4 to 0.6.
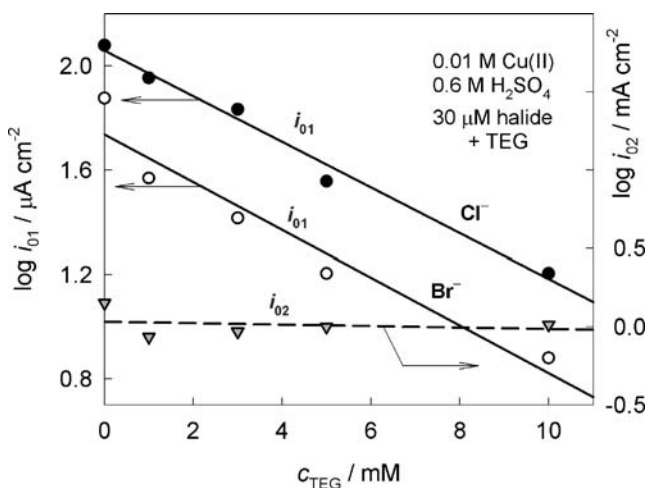
Fig. 3 Dependences of exchange current densities i_{01} (voltammetric data, ordinate to the left) and i_{02} (impedance data, ordinate to the right) on TEG concentration in solutions containing chlorides or bromides as indicated

Table 1 Influence of polyethylene glycols HO–(CH$_2$–CH$_2$–O–)$_m$H on kinetic parameters of the process $Cu^{2+} + e \rightarrow Cu^+$ in 0.01 M Cu(II) solutions containing 30 μM Br$^-$

PEG	m	c_{PEG}/mg dm^{-3}	α_{c1}	i_{01}/μA cm^{-2}
TEG (PEG-194)	4	0	0.39	120
		200	0.39	37
		600	0.38	26
		1,000	0.38	16
		2,000	0.39	7.6
PEG-300	6–7	10	0.46	11
		100	0.46	3
		200	0.49	0.7
PEG-600	13	1	0.69	0.25
		2	0.59	1.2
		5	0.54	1.1
		10	0.54	0.7
		50	0.53	0.5
PEG-3000	68	0.1	0.51	21
		0.2	0.45	6.5
		0.3	0.51	0.2
		0.5	0.47	0.2

Electroreduction of Sn(II)

Voltammograms of Sn(II) reduction in SAS-free solutions are simple in shape due to a rather high exchange current density that, according to different literature data, ranges from 50 to 250 mA cm^{-2}. However, the effect of PEG in this case is quite different than that observed for Cu(II) reduction: the SAS under discussion gives rise to a significant fall of current density in the entire range of cathodic polarizations. An inhibition of the cathodic process increases with the molecular mass of PEG. At the same time, the influence of the intensity of forced convection becomes weaker and the deviations from Levich behavior are observed (Fig. 4). Since the limiting current loses its diffusive nature, this circumstance caused us to abandon the NTP-based analysis of voltammetric data.

Another peculiarity consists in a rather slow adsorption of PEG on Sn substrate. This effect is typical of EG oligomers [18] and is notably pronounced at open-circuit conditions. It manifests itself in the significant rise of impedance with an exposure time τ of Sn electrode in the solution. It is worthy of note that such behavior, in particular, and adsorption ability, in general, is inherent to EG oligomers, beginning with TEG (Fig. 5). Initially, Nyquist plots are nothing else than lines with unit slope that is typical of diffusion-controlled processes. Further, the semicircle arises and develops with τ in the presence of surface-active PEGs, this being indicative of a decrease in i_0. For instance, in the case of solutions containing 5 mM of TEG, some rudiment of semicircle can be distinguished only at $\tau = 15$ min in the region of the highest frequencies ($3 < f < 50$ kHz). However, in the case of long-chain polyethers,
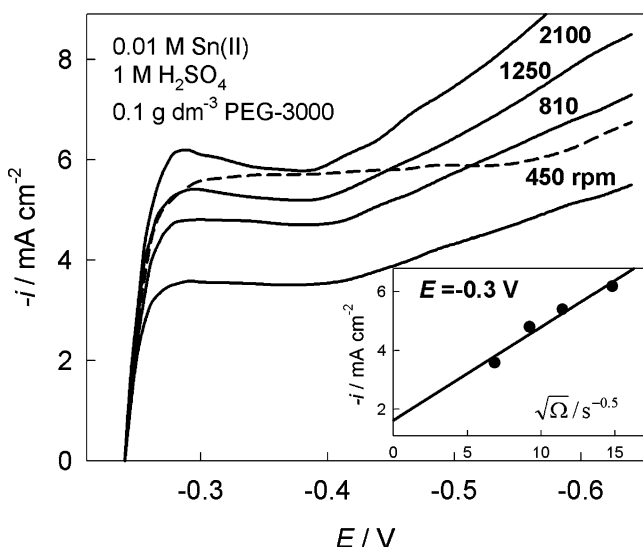
Fig. 4 Voltammograms of RDE obtained at different rotating velocities for 0.01 M Sn(II) solutions free of PEG (*dotted line*, 450 rpm) and with PEG-3000 (*solid lines*). Effect of the intensity of forced convection is shown in the *inset*

adsorption is stronger and equilibria in the adsorption layer are achieved significantly faster [10, 22, 23].

To describe quantitatively EIS data, the $R_\Omega([R_{ct}Q_d]Q_{dl})$ equivalent circuit was applied with the charge transfer resistance R_{ct} and constant phase elements (CPE) representing diffusion impedance Q_d and double-layer impedance Q_{dl}. This circuit fits the experimental data with frequency error less than 2%. As it is known, the admittance of CPE is given by relation: $Y=Y_0(j\omega)^n$. Time-independent parameters of Q_d were found to be as follows: $Y_0=0.37\pm0.02$ Ω^{-1} cm^{-2} s^n with $n=0.48\pm0.02$. The value of Warburg coefficient calculated for 0.01 M Sn(II) solution with $D=6.1\times 10^{-6}$ cm^2 s^{-1} is equal to 0.384 Ω^{-1} cm^{-2} s$^{0.5}$; it fairly coincides with the quantities of Y_0 established above. The exponent n obtained for Q_{dl} varies between 0.88 and 0.91, this being indicative of capacitive character of the double-layer impedance.

Exchange current densities were obtained from charge transfer resistances R_{ct} using well-known equation

$$i_0 = \frac{RT}{nFR_{ct}}. \qquad (9)$$

More than tenfold fall of i_0 (from ~70 to 6 mA cm^{-2}) and that of double-layer capacitance was observed after 2 h in 0.01 M Sn(II) solutions containing 20 mM of TEG. These effects seem to arise from the progressive saturation of the interface with adsorbed PEG, causing the increasing inhibition of tin reduction. Inhibition degree increases with PEG molecular: for PEG-3000, i_0 falls down to ~3 mA cm^{-2}.

To compare the effect of different polyethers with general formula: R−(CH$_2$−CH$_2$−O)$_m$−H, the values of i_0

were normalized in respect of "1 mol of ethereal oxygen." In other words, the i_0 values in the solutions involving the same amount of CH$_2$−CH$_2$−O− chains were correlated with PEG molecular mass. According to the results obtained, inhibition effect of molecules with 10–20 ethereal bonds is ~2,000 times higher as compared with TEG. Thus, the length of hydrocarbon chain is a prime factor responsible for inhibition activity of polyether on tin electrode.

Codeposition of copper and tin

Voltammograms in mixed 0.01 M Cu(II)–Sn(II) solutions contain two plateaus of limiting current. The first of them develops around $E=-0.2$ V and the second arises at −0.3 V. In the absence of SAS, both currents depend on the intensity of forced convection and obey Levich equation.

The effect of different PEGs is demonstrated in Fig. 6. When the length of hydrocarbon chain increases, voltammograms gradually lower and change their shape. Beginning with PEG-300, the characteristic voltammetric minimum originates at −0.24 V. Its depth depends both on PEG molecular mass and concentration, as well as on the intensity of forced convection (Figs. 7 and 8). In summary, it is possible to state that: (a) voltammetric minimum deepens and (b) the effect of forced convection weakens when the molecular mass of PEG grows. However, the minimum under discussion is larger and deeper when polyethers with branchy hydrocarbon chains are added [10, 23].

A sequence of partial processes is designated in Fig. 8. Despite the fact that the equilibrium potential of Sn|Sn^{2+} electrode $E_{eq}=-0.24$ V, the reduction of tin starts at ~0.0 V, i.e., UPD of tin is observed due to the formation of Cu–Sn
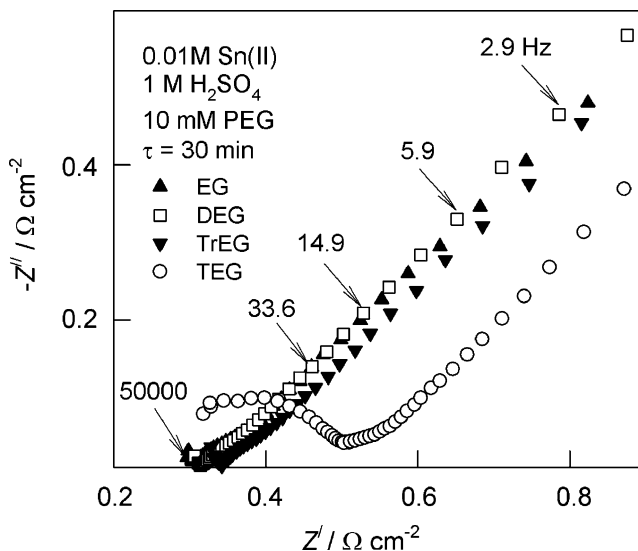
Fig. 5 Nyquist plots obtained for 0.01 M Sn(II) solutions containing 10 mM of different oligomers. Exposure time of Sn electrode $\tau= 30$ min. Applied frequencies in Hertz are given at some experimental points
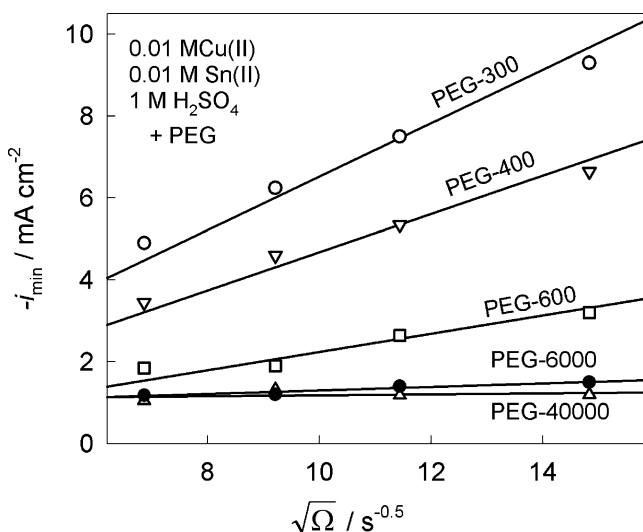
Fig. 6 Voltammograms obtained for 0.01 M Cu(II) + 0.01 M Sn(II) solutions containing 10 mM of indicated PEGs. Rotating velocity (rpm) is designated at the curves
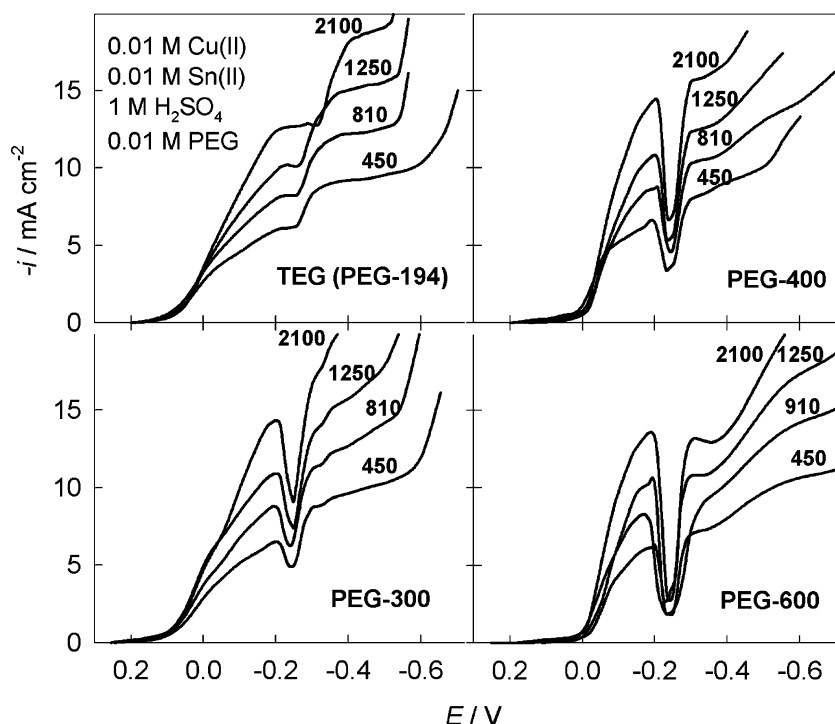

intermetalides in this region. Free-tin phase (β-Sn) is thermodynamically stable at $E<E_{eq}$ and the inhibitive adsorption of PEG is possible on Sn atoms that are not incorporated into common Cu–Sn lattice. This gives rise to a development of voltammetric minimum. Further increase in cathodic polarization results in the increase of the rate of codeposition, though the currents do not attain the values that are typical of SAS-free solutions. Desorption processes (at least, a partial destruction of the adsorption layer) are expected in this region.

Composition of Cu–Sn coatings deposited at different potentials may be seen from Table 2. A ~90-nm-thick layer was removed from the surface of samples before measurements. Content of tin slightly increases with PEG molecular mass at sufficiently low cathodic polarizations ($-0.14<E<-0.02$ V) where compact yellow bronze coatings are obtained. Powdery Cu–Sn deposits are formed in the region of voltammetric minimum and, again, quite good coatings of white bronze are obtained at −0.4 V.

Fig. 7 Minimum current densities plotted in Levich coordinates for 0.01 M Cu(II) + 0.01 M Sn(II) solutions containing 10 mM of PEG-300, PEG-400, or PEG-600 and 0.1 g dm⁻³ of PEG-6000 or PEG-40000
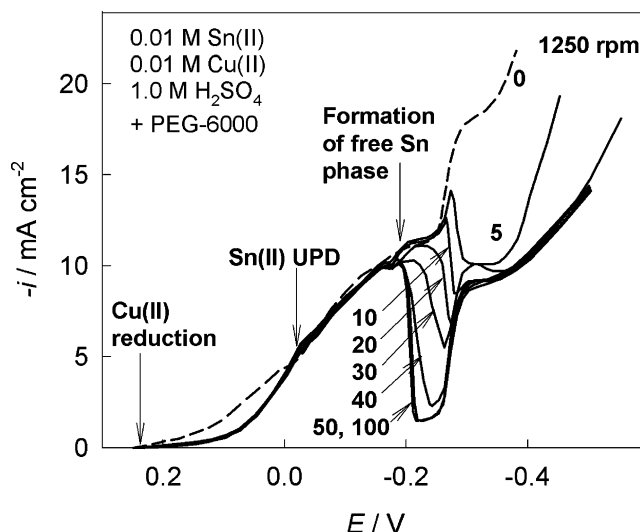
Fig. 8 Voltammograms obtained for 0.01 M Cu(II) + 0.01 M Sn(II) solutions containing PEG-6000, which concentration (mg dm⁻³) is indicated at the respective curves

Table 2 Content of tin (atomic percent) in the coatings obtained at different potentials in 0.01 M Cu(II) + 0.01 M Sn(II) solutions containing 0.1 g dm^{-3} of indicated PEG

	E/V			
	−0.02	−0.1	−0.14	−0.4
PEG-1000	2.8	5.6	7.9	62.8
PEG-6000	3.2	6.0	8.6	68.9
PEG-40000	3.8	6.6	8.9	82.2

The detected phenomena give grounds to suppose that PEG adsorption is the main factor responsible for inhibition of cathodic processes. From this point of view, voltammetric data might be treated invoking a simple kinetic model. According to it, the active and passive sites with different current densities are formed on the electrode surface due to PEG adsorption. Then, the surface coverage θ can be obtained from the relation

$$i = i_{\theta=0}(1 - \theta) + i_{\theta=1}\theta, \qquad (11)$$

where $i_{\theta=0}$ is the current density at $\theta=0$, i.e., in PEG-free solution, and $i_{\theta=1}$ concerns a fully saturated adsorption layer. The latter value was obtained by linear extrapolation of i_{min} values to $1/\sqrt{c_{PEG}} \to 0$. Validity of such procedure was evidenced in [23], where coinciding θ quantities were obtained from voltammetric and double-layer capacitance data.

Results obtained for PEG-1000 adsorption in voltammetric minimum are shown in Fig. 9, where θ values are fitted to Frumkin isotherm. A negative sign of parameter a shows that repulsive interaction between PEG molecules should prevail in the adsorption layer.

Summarizing the results obtained, it is possible to maintain that the inhibition degree increases with the length of PEG hydrocarbon chain. This conclusion is general for Cu(II) and Sn(II) reduction, though some nonessential deviations from this regularity were observed at comparatively low concentrations of long PEG molecules. To our opinion, the existence the minimal length of surface-active PEG molecule is the most interesting fact. Yokoi et al. [1] proposed that Cu$^+$ or Cu^{2+} ions coordinate with oxygen atoms of PEG and at the same time with Cl$^-$ ions adsorbed on Cu. Feng et al. [24] using SERS data demonstrated that the adsorption of PEG on the copper substance is associated with the presence of Cu$^+$ and Cl$^-$, where Cu$^+$ serves as an intermediate link between PEG and Cl$^-$. These images could serve as bases for further elaboration of the structure of adsorption layer. Talking of short PEG molecules (EG oligomers), namely, ethereal oxygen atoms seem to be responsible for interaction with electrode surface or other components of adsorption layer, whereas more hydrophilic OH groups should hamper such interactions. Therefore,

some critical number of ethereal oxygen atoms should exist in the SAS. The existence of three ethereal oxygen atoms in TEG molecule seems to create favorable conditions for the formation of pseudocrown complexes with adsorbed Cu$^+$ ions. The image of such cluster involving two PEG molecules was given in [17]. However, it is still unclear whether similar chemical interactions can occur between TEG and Sn^{2+} ions, though some potentiometric data are indicative of such possibility.

Conclusions

PEGs with different molecular mass were investigated in Cu|Cu^{2+} and Sn|Sn^{2+} systems. Tetraethylene glycol was found to be the surface-active oligomer on both Cu and Sn substrates that holds the shortest (–CH$_2$–CH$_2$–O–)$_m$ chain. Quantitative analysis of voltammetric data, transformed into normalized Tafel plots, shows that the exchange current density of the rate-limiting step Cu^{2+} + e → Cu$^+$ falls drastically with an increase in the molecular mass of PEG.

An addition of PEG into halide-free Sn(II) solutions results in the significant inhibition of Sn(II) reduction in the entire range of cathodic polarizations including the region of limiting current. Inhibition degree also increases with PEG molecular mass. In contrast with Cu|Cu(II) system, formation of adsorption layers on Sn electrodes proceeds slower and, in the case of short PEG molecules, can take some hours.

Underpotential deposition of Sn(II) is observed in the region of Cu(II)-limiting current at potentials that are more
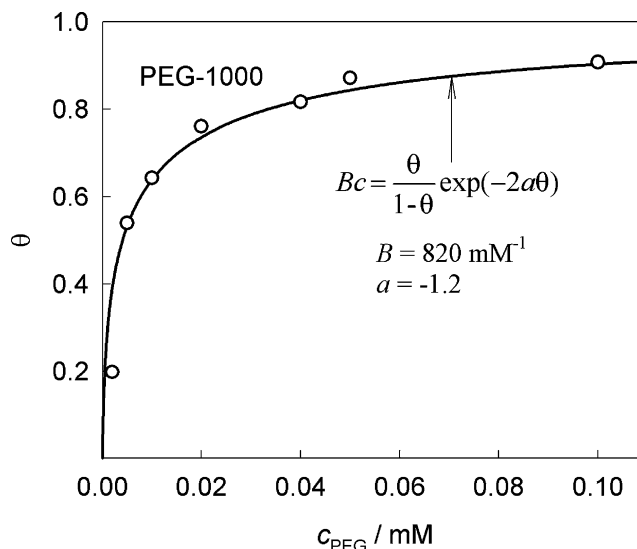
Fig. 9 Quasi-isotherm obtained for voltammetric minimum of 0.01 M Cu(II) + 0.01 M Sn(II) solutions containing PEG-1000. Experimental data (*circles*) are fitted to Frumkin isotherm (*line*)

positive than the equilibrium potential (E_{eq}) of Sn|Sn^{2+} electrode. Depolarization effects arise from the formation of intermetalides in the coatings. Formation of Sn phase at $E < E_{eq}$ gives rise to the characteristic current minimum that deepens with the length of the hydrocarbon chain of PEG. The fall of current density seems to be conditioned by the inhibitive PEG adsorption on tin atoms that are still not incorporated into general Cu–Sn lattice.

References

1. Yokoi M, Konishi S, Hayashi T (1983) Denki Kagaku 51:460
2. Healy JP, Pletcher D (1992) J Electroanal Chem 338:155 doi:10.1016/0022-0728(92)80420-9
3. Franklin TC (1994) Plat Surf Finish 4:62
4. Stoychev D, Tsvetanov CJ (1996) J Appl Electrochem 26:741 doi:10.1007/BF00241515
5. Kelly JJ, West AC (1992) J Electrochem Soc 145:3472, 3477
6. Jovič VD, Jovič BM (2001) J Serb Chem Soc 66:935
7. Bonou L, Eyraud M, Denoyel R, Massiani Y (2002) Electrochim Acta 47:4139 doi:10.1016/S0013-4686(02)00356-0
8. Hebert KR, Adhikari S, Houser JE (2005) J Electrochem Soc 152:C324 doi:10.1149/1.1882112
9. Survila A, Mockus Z, Kanapeckaitė S, Samulevičienė M (2003) Chemija Vilnius 14:30
10. Survila A, Mockus Z, Kanapeckaitė S (2003) J Electroanal Chem 552:97 doi:10.1016/S0022-0728(03)00047-0
11. Survila A, Mockus Z, Kanapeckaitė S, Jasulaitienė V (2004) Russ J Electrochem 40:855 doi:10.1023/B:RUEL.0000037952.60589.bd
12. Survila A, Mockus Z, Kanapeckaitė S, Samulevičienė M (2003) Chemija (Vilnius) 14:35
13. Reid JD, David AP (1987) Plat Surf Finish 74:66
14. Pearson T, Dennis JK (1990) J Appl Electrochem 20:196 doi:10.1007/BF01033595
15. Dow W-P, Yen M-Y, Lin W-B, Ho S-W (2005) J Electrochem Soc 152:C769 doi:10.1149/1.2052019
16. Bražinskienė D, Survila A (2005) Russ J Electrochem 41:979 doi:10.1007/s11175-005-0166-0
17. Bražinskienė D, Survila A, Samulevičienė M (2005) Chemija Vilnius 16:20
18. Survila A, Bražinskienė D (2007) J Solid State Electrochem 11:65 doi:10.1007/s10008-005-0070-2
19. Boukamp BA (1989) Equivalent circuits (EQUIVCRT.PAS), users' manual. University of Twente, Netherlands
20. Survila A, Mockus Z, Kanapeckaitė S, Jasulaitienė V, Juškėnas R (2007) Electrochim Acta 52:3067 doi:10.1016/j.electacta.2006.09.040
21. Survila A, Baliukienė V (2001) Chemija Vilnius 12:195
22. Survila A, Mockus Z, Kanapeckaitė S (2002) Trans IMF 80:85
23. Survila A, Mockus Z, Kanapeckaitė S, Samulevičienė M (2005) Electrochim Acta 50:2879 doi:10.1016/j.electacta.2004.11.034
24. Feng ZV, Li X, Gewirth AA (2003) J Electrochem Soc 107:9415